Summary: Laser-induced fluorescence spectroscopy of the optical probe Nile Blue A in polymer clay nanocomposites is described. Concentration quenching of the fluorescence dominates the probe behavior until the clay platelets are physically separated by polymer intercalation. Further separation into an exfoliated structure results in an intense increase in probe fluorescence. Preliminary results indicate the ability to discriminate between intercalated and exfoliated structures in nanocomposites formed by melt processing.

Polyamide 6 nanocomposites: Purple, 1 minute processing (left). Red, 7 minute processing (right).

Optical Probes for Monitoring Intercalation and Exfoliation in Melt-Processed Polymer Nanocomposites

*Paul H. Maupin,**[1a] *Jeffrey W. Gilman,*[2] *Richard H. Harris, Jr.,*[2] *Severine Bellayer,*[2b] *Anthony J. Bur,*[3] *Steven C. Roth,*[3] *Marius Murariu,*[4] *Alexander B. Morgan,*[5] *Joseph D. Harris*[5]

[1] Office of Basic Energy Sciences, Office of Science, U.S. Department of Energy, Washington, DC, USA 20585
Fax: (+1) 301 903 4110; E-mail: paul.maupin@science.doe.gov
[2] Building and Fire Research Laboratory, National Institute of Standards and Technology, Gaithersburg MD, 20899, USA
[3] Materials Science and Engineering Division, National Institute of Standards and Technology, Gaithersburg MD, 20899, USA
[4] Materia Nova-Service des Materiaux Polymeres et Composites, Universite de Mons, B 7000, Mons, Belgium
[5] Dow Chemical Company, Midland, MI, USA

Received: November 17, 2003; Revised: December 23, 2003; Accepted: January 5, 2004; DOI: 10.1002/marc.200300262

Keywords: extrusion; fluorescence; nanocomposites; Nile Blue A; organoclay

Introduction

Interest in polymer-clay nanocomposites has increased due to their improved mechanical properties, barrier properties, lower water absorption, and reduced flammability. Many of the desirable properties of polymer nanocomposites are related to the quality of the nano-dispersion, including polymer intercalation into the clay galleries and/or exfoliation (delamination) into individual clay platelets.[1,2] Unfortunately, the methods available to characterize the processing effectiveness require laborious offline testing of samples by methods such as X-ray diffraction (XRD), transmission electron microscopy (TEM), and solid-state nuclear magnetic resonance (NMR).[3–6] Recently, the use of fluorescent probes has been reported to monitor resin temperature in polymer injection molding and temperature gradients in an extruded resin flow stream.[7,8] Other optical methods require the probing light to transmit through the material, but fluorescence measurements can be carried out by excitation and detection from one side only. In these

[a] Guest researcher at the National Institute of Standards and Technology and the Naval Research Laboratory.
Disclaimer: This work was carried out by the National Institute of Standards and Technology (NIST), an agency of the U. S. government, and by statute is not subject to copyright in the United States. The identification of any commercial product or trade name does not imply endorsement or recommendation by the National Institute of Standards and Technology.
[b] Guest researcher at the laboratory GEMTEX of Ecole Nationale des Arts et Industries Textiles (ENSAIT), Roubaix, France.

applications the thermal stability of the fluorescent probe is of paramount importance since typical processing conditions involve temperatures between 200 and 300 °C.

The most common layered silicate used in polymer-clay nanocomposites is montmorillonite (MMT).[9] It consists of clay layers stacked upon each other with a ''deck of cards'' -like registry. The gap between the clay layers is referred to as the gallery spacing (or $d(100)$ spacing) and is dependent on the size of the species intercalated in the clay gallery. The clay layers have a net negative charge compensated by Na^+ or K^+ ions in the gallery space. In the natural state, MMT clay does not disperse or exfoliate in most polymers. Exchange of the natural cations with an organic modifier (normally an organic cation such as dimethyl di(hydrogenated tallow) ammonium cation) increases the gallery spacing (1.7 nm to 3.0 nm) and improves the polymer and clay interactions; this, in turn, leads to a higher degree of organoclay dispersion and exfoliation.

Cationic optical probes adsorb strongly on clay mineral surfaces and their intermolecular interactions and surface organizations are complex functions of the concentration, stoichiometry (as a fraction of the cation exchange capacity CEC), and charge density. Dye-aggregate formation is common and their type is controlled by the density of negatively charged sites at the clay surface.[10] Common aggregates are H-type (head-to-head), J-type (head-to-tail), and higher order aggregates. Various amounts of dye monomers, dimers, and higher aggregates result at the surface. Aging dye-clay dispersions results in the redistribution and intercalation of smaller species into the clay galleries.[11] It is now recognized that clay-dye suspensions slowly reach thermodynamic equilibrium and dye organization depends on a subtle balance of several forces and properties of the adsorbates and surfaces.[12]

The photofunctions of optical probes in intercalation compounds have been a topic of great interest.[13] Various cationic fluorescent dyes have been studied that show a dependence of the fluorescence intensity on the type of clay and concentration as a fraction of the exchange capacity. Clays such as natural MMT contain a substantial portion of iron in their octahedral layers, which leads to quenching of fluorescence. Concentration quenching can also occur at higher levels of probe concentration.[14] Intercalation of a cationic coumarin dye into a swelling clay containing no iron extended the dye's thermal stability to 300 °C and resulted in a red shift to longer wavelength for the fluorescence emission.[15] In contrast, the cationic laser dye Nile Blue A (NB) in ethanol in uncharged porous sol-gel glasses shows Stokes shift decreases as a function of nano-confinement and fluorescence blue shifts below confinements of 7.5 nm.[16] Nano-confinement in 5 nm pores in the nonpolar medium dodecane leads to a more pronounced blue shift from 664 nm (ethanol) to 648 nm. NB forms aggregates upon interaction with negatively charged colloidal silica.[17] These colloids are not layered and cause the surface formation of nonfluorescent H-type aggregates comprised of NB dimer units. NB also exhibits acid-base behavior. Deprotonation of NB to Nile Blue Base causes a blue shift of the fluorescence from 675 nm to 580 nm in basic media like triethylamine.[18] The complex photo properties of NB makes it a sensitive probe of the local nano-environment.

This communication describes an approach for the rapid analysis of intercalation and exfoliation in melt-processed polymer-clay nanocomposites based on laser-induced fluorescence (LIF) spectroscopy of optical probes. Preliminary findings are reported on probe fluorescence in polymer nanocomposites prepared from organically modified MMT and polystyrene (PS) and polyamide-6 (PA-6). We find Nile Blue A to be a useful fluorescence probe when co-exchanged into MMT with traditional quaternary ammonium treatments or advanced, high temperature stable trialkylimidazolium treatments.[19,20]

Experimental Part

Preparation and Characterization of Organically Modified Layered Silicates

Standard ion-exchange procedures using aqueous ethanol were modified.[21] Sodium cloisite, a natural montmorillonite with an ion-exchange capacity of 92 meq/100 g was obtained from Southern Clay Products (Gonzales, Texas). 1,2-Dimethyl-3-hexadecylimidazolium (DMHDIM) bromide was prepared and purified as described previously.[19] Dimethyl dioctadecylammonium (DMDODA) bromide, Nile Blue A Perchlorate, and Methylene Blue (MB) were obtained from the Aldrich Chemical Company and were used as received. Briefly, the appropriate ratios of the optical probe and DMHDIM or DMDODA salts necessary to achieve complete exchange were dissolved in 50 mL of hot ethanol-water (95%, Wherever % is used in this manuscript it means mass fraction %). Sodium cloisite (5 g) was added with rapid stirring until the solid was well dispersed. The volume was adjusted to 100 mL. with distilled water then stirred and heated for one hour at about 70 °C. It was then allowed to stand in a dark cabinet for three to seven days. The exchanged clay was filtered, washed with hot 50% ethanol-water, and then 95% ethanol until the filtrate was colorless. The resulting clays were dried at 100 °C in a forced convection oven for one hour then finely ground.

The clays were characterized by XRD and thermogravimeteric analysis (TGA). TGA data were collected from 30 °C to 800 °C at 10 °C/min under an N_2 atmosphere (samples 5–10 mg each) using a TA Instruments SDT 2960. XRD data were collected on a Philips diffractometer using $Cu_{K\alpha}$ radiation. The d spacing has an uncertainty of 0.03 nm (2σ) as determined by running a standard sample of NaMMT several times.

Preparation and Characterization of the Nanocomposites

PS and PA-6 nanocomposites were prepared in a mini-twin-screw melt extruder (intermeshing, conical, DACA Corp.).

Polymer and treated MMTs were charged into the mini-extruder and mixed at 21 rad/s (200 rpm) for variable times (1–7 min) and processing temperatures (180 °C to 240 °C). Commercial polymers containing no fillers were employed. PS was Styron 663 (Dow Chem. Corp.). PA-6 was UBE Corp. 1015B.

The nanocomposites were characterized by XRD and LIF. Selected samples were characterized by TEM using techniques described previously.[19] Fluorescence spectra were obtained using an Ocean Optics USB2000 spectrometer adapted for fiber optic input with a 200 μm entrance slit width. Several light sources were evaluated: a Thermo-Oriel xenon arc lamp filtered at 365 nm, a 407 nm Power Technologies diode laser, an air-cooled argon-ion laser tuned to 454 nm and 514 nm (OmniChrome model 171B), and a Spectra-Physics helium-neon laser at 632 nm. A bifurcated optical fiber containing seven fibers of 200 μm core diameter was used for both excitation and collection. Excitation light was transmitted through one fiber and focused onto the sample surface with a spot size of 0.5 mm diameter. The other six fibers collected fluorescence and transmitted it to the spectrometer. Integration times ranged between 500 ms and 6 s. All measurements were made at room temperature on strands from the extrusion.

Results and Discussion

Thermal Stability of Optical Probes in Layered Silicates

The thermal stabilities of the optical probes were evaluated by preparing ion-exchanged MMT samples where a 9:1 ratio of organic modifier to probe was used to completely exchange the Na^+. TGA results (not shown) indicated that NB and MB had sufficient thermal stability for preparing melt-processed nanocomposites. Their thermal stabilities were not significantly different to those with the organic treatments alone.[19] DMHDIM-MMT samples had high thermal stability (350 °C onset), which is important for melt processing high-melting-temperature polymers such as PA-6. DMDODA-MMT samples had adequate thermal stability (250 °C onset) for processing polymers such as PS.

Fluorescence and Melt Processing Studies

The usefulness of NB and MB as probes was evaluated by preparing a series of nanocomposites with PS and PA-6. The intercalation and exfoliation behavior of PS and PA-6 with DMHDIM-MMT has been well established and depends on the processing time and temperature.[19] The PS nanocomposites are a mixed intercalated-exfoliated structure dominated by intercalation. The PA-6 nanocomposites exhibit a highly exfoliated structure.

Background spectra (Figure 1) show the effect of the NB level on clay fluorescence. Concentration quenching dominates above the 1% CEC probe level. Several broad emission bands at 511, 588, and 655 nm are evident in the 0.5% NB CEC level sample with emissions shifted in accordance with surface adsorption effects and the formation of dimers and higher aggregates.

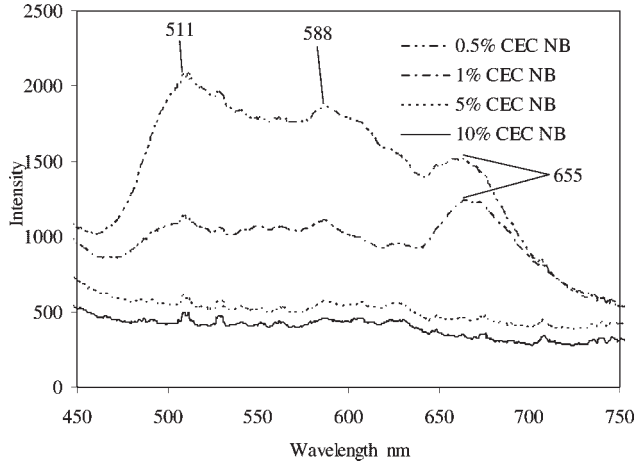

Figure 1. LIF spectra of NB/DMHDIM-MMT at different levels of NB. 407 nm excitation wavelength, 4 s integration.

In initial extrusion studies only the experiments performed with NB/DMHDIM-MMT showed any fluorescence. Additional studies with higher processing temperatures revealed that the appearance of fluorescence was a general phenomenon depending on the probe and the nanocomposite system. NB was the most uniformly useful optical probe useful in both polymer media evaluated. MB showed fluorescence in only one case where the organic treatment was DMDODA. Enhanced second-order nonlinear optical behavior has been observed for MB adsorbed on Laponite, a synthetic clay that does not contain iron impurities.[22]

The NB melt dispersed in PS (Figure 2) exhibits emissions at 498 and 651 nm when excited at 407 nm. The PS

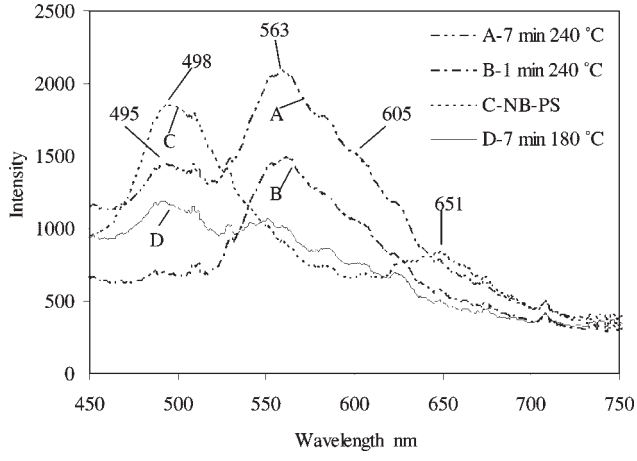

Figure 2. LIF spectra (ex = 407 nm, 6 s integration) of PS nanocomposites with 2% NB/DMHDIM-MMT (NB level 10% CEC) at different processing temperatures and residence times and a melt dispersion of NB in PS (180 °C).

nanocomposite extrusion at sub-optimal temperatures exhibits no fluorescence at one minute (not shown) and the appearance of weak emissions at 495 nm and 563 nm for seven-minute processing. A higher processing temperature (240 °C) at one-minute residence results in the appearance of the 563 nm band with significant fine structure at longer wavelengths. This emission is more pronounced at longer processing times and the low wavelength emission grows in intensity. The fine structure above the 563 nm band appears to have a periodic order of approximately 20–24 nm. The XRD data of these samples (not shown) yield very little detailed information on the evolution of the PS nanocomposite structures.

In PA-6 nanocomposites (Figure 3) the lowest processing time gives a broad emission around 565 nm with a significant contribution from a shoulder at higher wavelengths. The longer processing time shows a large increase in intensity dominated by a band around 605 nm. The periodic step function-like fine structure observed in the PS nanocomposites was not observed. Additionally, a weak band appears at low wavelength (502 nm) as in the PS nanocomposite. The NB melt dispersed in PA-6 exhibits very weak fluorescence at 678, 608, and 498 nm. XRD data (not shown) suggest that some of the layered silicate structure, with the original d-spacing, remains in the sample processed for 1 min.

Our data interpretation assumes subsidence of quenching in the nanocomposite and emission wavelengths that depends on the nano-confinement and the local environment. For exfoliation and clay-sheet separations approaching 7.5 nm, NB emissions for an unconfined hydrophobic environment are expected.[16] TEM of the nanocomposites (Figure 4) shows evolution into a predominately intercalated structure with large tactoids for the PS nanocomposite system at the 240 °C, 7 min. processing condition, and a well-exfoliated structure for the PA-6 system under the same processing conditions. Comparison of the emissions in the PA-6 nanocomposite with XRD and TEM data suggests that the emission at 565 nm is related to intercalation and that at 605 nm is indicative of exfoliation. These same bands are present in the PS nanocomposite spectra, where intercalation dominates. The actual emission wavelengths appear to be insensitive to the polymer polarity, suggesting that the dye is tightly bound in the hydrophobic environment of the treated silicate. The 20–24 nm step function increments for wavelengths above 563 nm in the PS nanocomposite are intriguing. With higher resolution it

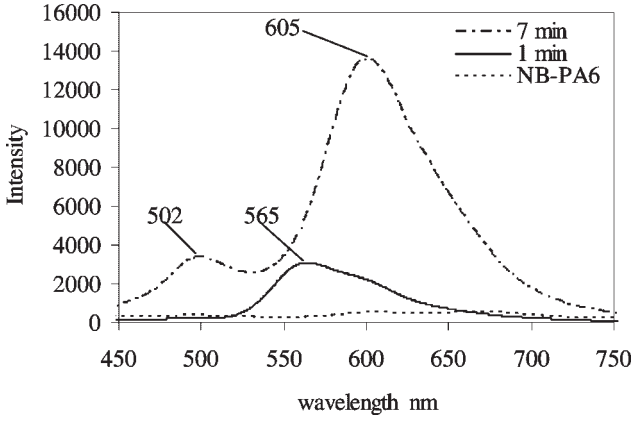

Figure 3. LIF spectra (ex = 407 nm, 800 ms integration) of PA-6 nanocomposites with 2% NB/DMHDIM-MMT (NB level 10% CEC) processed at 240 °C and different residence times and a melt dispersion of NB in PA-6 (240 °C, 1 s integration).

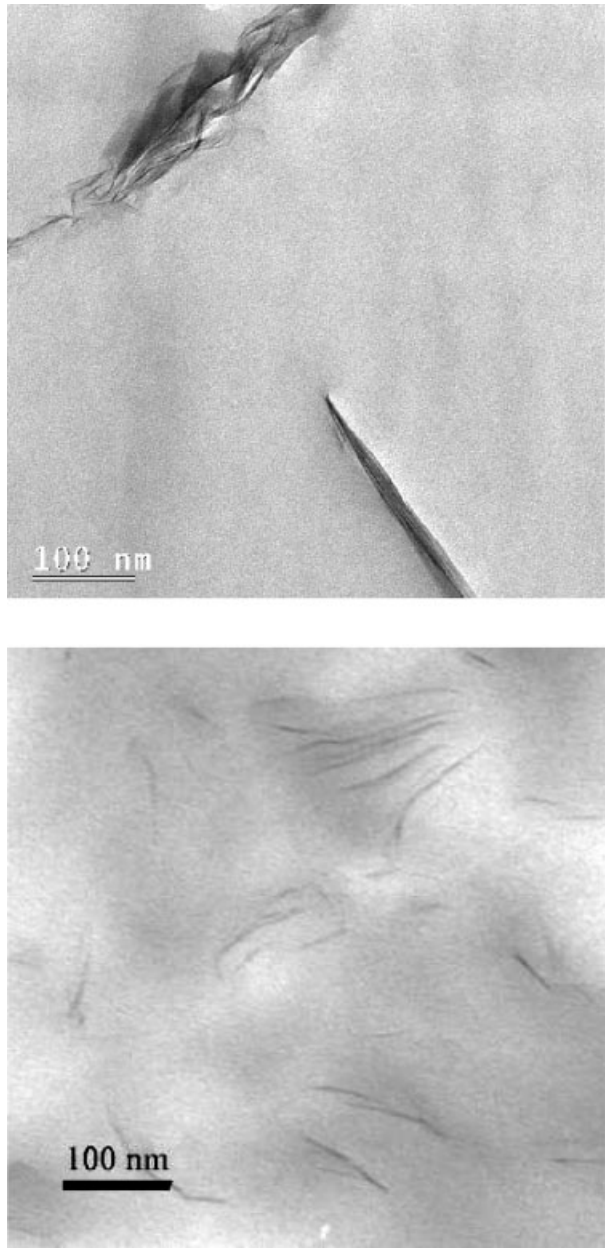

Figure 4. TEM images of representative 2% NB/DMHDIM-MMT (NB level 10% CEC) nanocomposites. PS: 7 min processing at 240 °C (top). PA-6: 7 min processing at 240 °C (bottom).

may prove possible to monitor the stepwise evolution of an intercalated nanocomposite structure into an exfoliated structure. The nature of the emission around 495–502 nm is less clear and could be explained by desorption of NB into the polymer matrix, or from unquenched higher-order aggregates on the clay. Finally, the visible colors of the polymer nanocomposite structures changed during the processing as well. The PS samples generally retained the color of the parent probe, whereas the PA-6 samples changed from shades of magenta to bright red as the processing times increased.

Conclusion

This publication reports the fluorescence behavior of optical probes in polymer nanocomposites. Preliminary results indicate that NB, a cationic laser dye, is well suited to probe nano-confinement in polymer nanocomposites. The appearance and relative intensity of fluorescence is ascribed to decreased quenching in the nanocomposite. The emission wavelengths depend on local nanostructure, where confinements below 7.5 nm result in significant blue shifts. Comparison with other characterization techniques allows the correlation of polymer intercalation with emissions centered about 565 nm and exfoliation into individual platelets surrounded by the polymer matrix with emissions at 605 nm and higher.

The broad separation of emission wavelengths should allow for the development of methods to assess the detailed nanostructure and quality of polymer nanocomposites formed by melt processing. It may be possible to use this approach as a quantitative tool once a thorough understanding of the probe's optical behavior in polymer nanocomposites is achieved. It is also likely that these same methods will be useful for studying polymer nanocomposites made by other methods of formation. We will continue to explore the optical behavior of fluorescent probes in polymer nanocomposites. Their UV-Visible spectroscopic behavior will be studied and reported elsewhere. Use of this method of characterization will also be applied to on-line monitoring of nanocomposites during extrusion.

Acknowledgements: We thank *Professor Serge Bourbigot* for helpful discussions. The author acknowledges the *Air Force Office of Scientific Research* for funding, *NIST* and the *Naval Research Laboratory* for use of their facilities and equipment, and the *DOE Office of Science* for permission to engage in active research.

[1] M. Alexandre, P. Dubois, *Mater. Sci. Eng. R.* **2000**, *28*, 1.
[2] S. S. Ray, M. Okamoto, *Prog. Polym. Sci.* **2003**, *28*, 1539.
[3] D. L. VanderHart, A. Asano, J. W. Gilman, *Macromolecules* **2001**, *34*, 3819.
[4] D. L. VanderHart, A. Asano, J. W. Gilman, *Chem. Mater.* **2001**, *13*, 3781.
[5] D. L. VanderHart, A. Asano, J. W. Gilman, *Chem. Mater.* **2001**, *13*, 3796.
[6] A. B. Morgan, J. W. Gilman, *J. Appl. Polym. Sci.* **2003**, *87*, 1329.
[7] A. J. Bur, M. G. Vangel, S. Roth, *Appl. Spectr.* **2002**, *56*, 174.
[8] K. B. Migler, A. J. Bur, *Polym. Eng. Sci.* **1998**, *38*, 213.
[9] E. P. Giannelis, *Adv. Mater.* **1996**, *8*, 29.
[10] J. Bujdak, N. Iyi, *Clays Clay Miner.* **2002**, *50*, 446.
[11] J. Bujdak, M. Janek, J. Madejova, P. Komadel, *J. Chem. Soc., Faraday Trans.* **1998**, *94*, 3487.
[12] R. A. Schoonheydt, *Clays Clay Miner.* **2002**, *50*, 411.
[13] M. Ogawa, K. Kuroda, *Chem. Rev.* **1995**, *95*, 399.
[14] R. A. Schoonheydt, P. Depaum, D. Vliers, F. C. DeSchrijer, *J. Phys. Chem.* **1984**, *88*, 5113.
[15] T. Endo, N. Nakada, T. Sato, M. Shimada, *J. Phys. Chem. Solids* **1989**, *50*, 133.
[16] R. Baumann, C. Ferrante, F. W. Deeg, C. Brauchle, *J. Chem. Phys.* **2001**, *114*, 5781.
[17] C. Nasr, S. Hotchandani, *Chem. Mater.* **2000**, *12*, 1529.
[18] A. Dougal, *J. Phys. Chem.* **1994**, *98*, 13131.
[19] J. W. Gilman, W. H. Awad, R. D. Davis, J. Shields, T. Kashiwagi, D. L. VanderHart, R. H. Harris, Jr., C. Davis, A. B. Morgan, T. E. Sutto, J. Callahan, P. C. Truelove, H. C. Delong, *Chem. Mater.* **2002**, *14*, 3776.
[20] F. A. Bottino, E. Fabbri, I. L. Fragala, G. Malandrino, A. Orestano, F. Pilati, A. Pollicino, *Macromol. Rapid Commun.* **2003**, *24*, 1079.
[21] T. Endo, T. Sato, M. Shimada, *J. Phys. Chem. Solids* **1986**, *47*, 799.
[22] C. Boutton, M. Kauranen, A. Persoons, M. P. Keung, K. Y. Jacobs, R. A. Schoonheydt, *Clays Clay Miner.* **1997**, *45*, 483.

